PŮVODNÍ PRÁCE/ORIGINAL PAPER

Petrography and mineral chemistry of metaultramafics in the Austroalpine Sieggraben structural complex at Sieggraben and Schwarzenbach, Austria

Samila Hrvanović, Marián Putiš* and Peter Bačík

*Department of Mineralogy and Petrology, Faculty of Natural Sciences, Comenius University, 842 15 Bratislava, Slovak Republic, *e-mail: putis@fns.uniba.sk*

Hrvanović S., Putiš M., Bačík P. (2014) Petrography and mineral chemistry of metaultramafics in the Austroalpine Sieggraben structural complex at Sieggraben and Schwarzenbach, Austria. *Bull. mineral.-petrolog. Odd. Nár. Muz. (Praha) 22, 1, 105-114. ISSN 1211-0329.*

Abstract

The Sieggraben structural complex occupies a middle position (the former Middle Austroalpine Unit) in the Austroalpine basement nappe system in the Eastern Alps. It is reported as a part of the Upper Austroalpine Unit and is located in the Rosalien Mountains between the Sieggraben and Schwarzenbach villages (approximately 80 km south of Vienna). Our main goal is to precisely determine the petrography and mineral chemistry of lensoidal metaultramafic bodies in metapelites (micaschists to gneisses, migmatitic gneisses), metabasites (eclogites, amphibolites, metagabbros), impure metacarbonates to calc-silicate rocks (marbles), crosscut by veins of granitic orthogneisses (leucocrate metagranites, metapegmatites) in a pre-Alpine basement complex. Mineral assemblages from representative microstructures of massive to strongly schistose metaultramafics were studied by polarized-light microscopy and mineral chemical compositions were determined by Cameca SX-100 electron microprobe. Part of the metaultramafics preserves a mineral assemblage characterized by a higher content of olivine (forsterite) and orthopyroxene (enstatite) relics from the inferred eclogite facies metamorphic stage (D1). Antigorite, Ca-amphibole (tremolite) and Mg-rich chlorite (1) with chromite as the main matrix in the exhumation amphibolite facies metamorphic stage (D2); and chrysotile, Mg-rich chlorite (2), magnetite, rare talc and carbonates in the greenschist facies metamorphic stage (D3). Clinopyroxene is absent. The studied metaultramafics are mantle fragments emplaced in a subducted continetal crust most likely due to the Cretaceous subduction-collision event reported from this basement.

***Key words**: Sieggraben structural complex, metaultramafics, petrography, mineral chemistry*

Received: 1. 2. 2014; accepted: 17. 6. 2014

Introduction

Eclogite-bearing complexes provide information on subducted rocks, recrystallization P-T conditions and also on mineral deformation mechanisms in a subduction channel or accretionary wedge. Both mantle rocks and continental and/or oceanic crustal rocks are typical members of subduction complexes therefore interactions between these rock types provide important information on subduction and exhumation mechanisms.

The Sieggraben structural complex in the Rosalien Mountains at the south-eastern margin of the Eastern Alps contains metaultramafics in an eclogite-bearing basement complex. According to Tollmann (1980), the Sieggraben structural complex is a part of the Middle Austroalpine tectonic unit in the Eastern Alps (Fig. 1). Although this complex is most likely a remnant of a pre-Alpine basement, it has a strong Alpine polyphase metamorphic/deformational overprint (Putiš et al. 2000, 2002).

The geological and geotectonic evolution of this complex was characterized by Tollmann (1980), Frank et al. (1987), Frisch and Neubauer (1989), Neubauer et al. (1992), Neubauer and Frisch (1993) and Neubauer (1994). The results of isotopic mineral and whole-rock dating were described by Dallmeyer et al. (1992, 1996), Thöni and Jagoutz (1993), Froitzheim et al. (1996) and Putiš et al. (2000); all reporting Alpine metamorphic overprint.

Data on its geological mapping, petrotectonics and petrology was supplied by Putiš and Korikovsky (1993, 1995), Korikovsky et al. (1998) and Putiš et al. (1994, 2000, 2002). While petrological and geothermobarometric data, including the evolutionary P-T pathway of the host eclogite-bearing complex was suggested by Putiš et al. (2002) and Kromel et al. (2011), its metaultramafics have never been investigated in detail.

The metaultramafics in this Austroalpine (AA) Sieggraben structural complex (SSC) occur as lenses in eclogite facies metamorphic rocks. They are mantle fragments which enable reconstruction of the tectonometamorphic evolution and allow identification of crust-mantle interactions. This paper presents new petrographic and mineral chemical data from metaultramafics sampled between Sieggraben and Schwarzenbach (Fig. 2), and their evolutionary stages are compared with those published for host eclogite facies rocks in this area.

Geological setting

The tectonostratigraphy of the AA structural complexes is based on the work of Tollmann (1980). Schmid et al. (2004) avoided Middle AA Unit terminology; considering this part of the Upper Austroalpine (UAA) Unit.

The top of the tectonostratigraphic profile has UAA SSC (sensu Schmid et al. 2004) overlaying the Lower Austroalpine (LAA) Grobgneiss and Wechsel structural

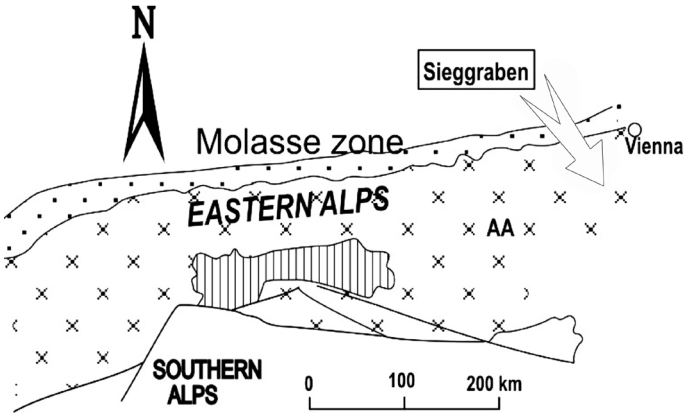

Fig. 1 *Location of the Sieggraben structural complex in the Austroalpine basement. Geographic coordinates of the sampling sites: Sieggraben area samples S-200a4, S-200e, S-200f3, S-201, S-201-2a, S-201-2b (N 47° 66' 75", E 16°36' 92") and Schwarzenbach area samples SW-3-1, SW-3-2, SW-4-1-2a, (N 47°64' 80", E 16°35' 47").*

Fig. 2 *Geological map of the Sieggraben structural complex and its surrounds (Putiš 1995, from Putiš et al. 2002).*

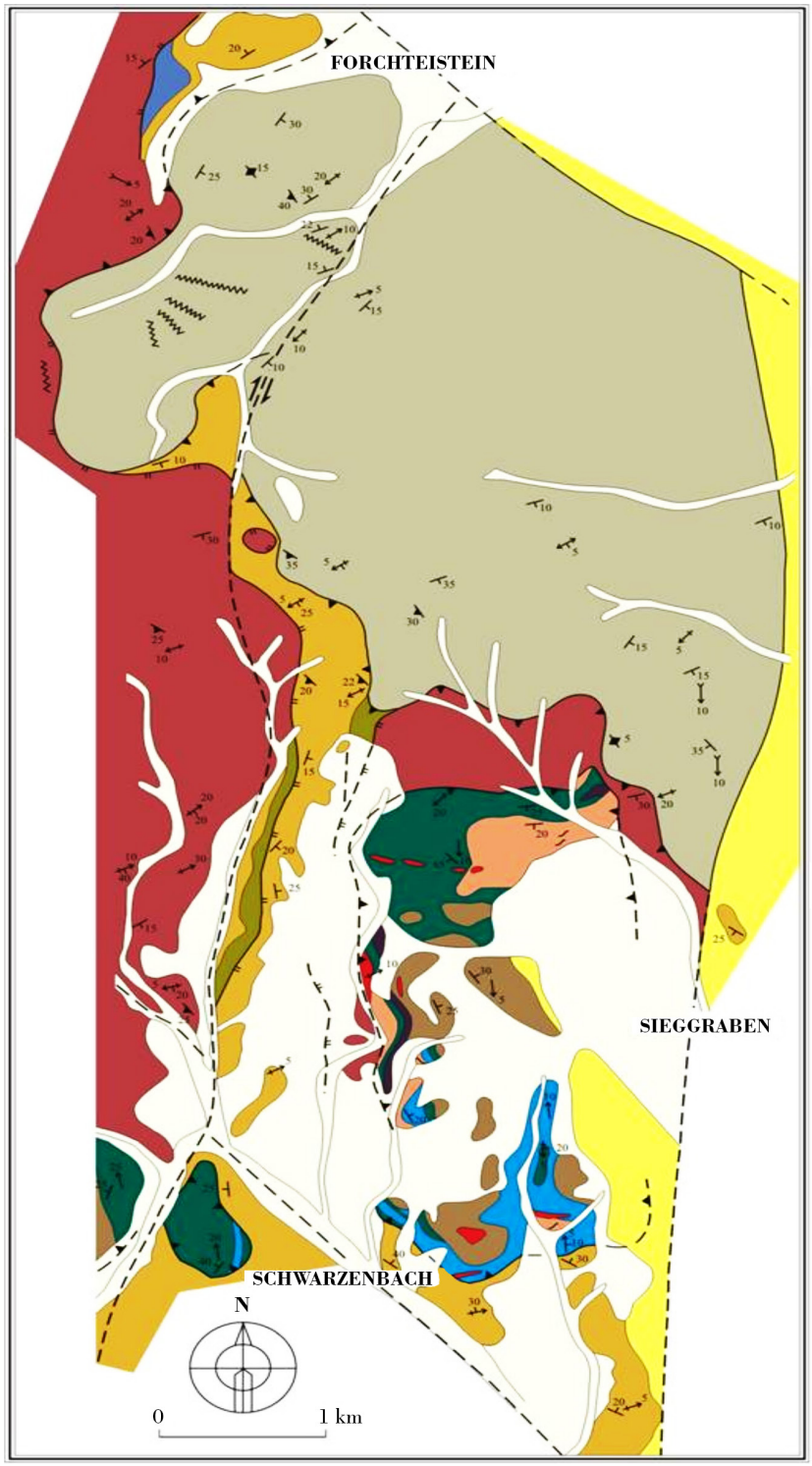

Geological map of the Sieggraben area (Eastern Alps)

(M. PUTIŠ 1995)

1 Quaternary

2 Neogene (a) Mesozoic (b)

SIEGGRABEN UNIT (Middle Austroalpine)

3 Sil-Ky paragneisses eyed, banded gneisses

4 Ms-Bt micaschists (a) Ms-Bt-Am-calcsilicates (b)

5 marbles, erlans

6 serpentinites

7 eclogites, amphibolitized eclogites, amphibolites, banded amphibolites

8 metapegmatitoids, metaaplitoids, metagranites

GROBGNEIS UNIT (Lower Austroalpine)

9 paragneisses, amphibolites

10 metagranitoids

11 metaconglomerates

WECHSEL UNIT (Lower Austoalpine)

12 phyllites, quartzites

TECTONIC STRUCTURES

13 thrust

14 reverse fault

15 fault tectonic boundary

16 25 metamorphic foliation; S-planes in sheared metagranitoids of SC-types

17 30 mylonitization and phyllonitization planes; C-planes od SC-types of mylonites

18 10 middle temparatura mineral-stretching lineation (in amphibolite facies)

19 5 low temperature (extensional) stretching lineation (in greenschist facies)

20 10 crenulation lineation (B-axes of crenulation folds)

21 quartz vein systems

complexes as a result of the Cretaceous collisional event (Neubauer 1994).

The crystalline basement rocks incorporated in the SSC are a part of the Koriden terrane (Frisch, Neubauer 1989; Neubauer, Frisch 1993), forming an accretionary wedge originally derived from the flyschoid sediments and the ocean fragments near a trench located on the upper northern Variscan plate (Matte 1986, 1991; Putiš et al. 2000).

Field geological-structural mapping determined two main types of thrust-faults and related meso- and microstructures in the Sieggraben area (Putiš et al. 2000, 2002).

Early Cretaceous higher-temperature structures are defined by NNW - SSE trending high-pressure D1 mineral lineations recorded in high-pressure phases of Cpx-Omp, Zo and Amp-Prg, and also in the mostly medium-temperature D2 lineations of Qz, Pl, Amp in ductile layered mylonites. These higher-temperature structures are recognizable only in the internal parts of the AA SSC, and they are overprinted by D3 lower temperature WSW dipping stretching lineations in ductile blastomylonitic/phyllonitic microstructures; particularly evident in the hanging wall.

Overprinting low-angle normal faults, most likely active during late Cretaceous to Early Neogene, were observed in the footwall of the SSC and the underlying LAA Grobgneis structural complexes (the latter overlying the deeper LAA Wechsel structural complex). Top-to-WSW movement along the low-temperature lineation is defined by linear orientation of newly formed fine-grained white mica aggregates (Ms), Bt and Chl. These are combined with asymmetric S-C type microstructures in metapelites and orthogneisses.

The pre-Alpine metamorphic age here is presumed Paleozoic. This is inferred from the U/Pb upper intercept age of zircon, apatite and monazite at 312.7±7.9 Ma, and/or the whole-rock Rb/Sr isotope age of 289±16 Ma, dating the granitic protoliths of the Sieggraben orthogneisses (Putiš et al. 2000). These dates indicate the magmatic age of an orthogneiss granitic precursor which intruded an Early Paleozoic metamorphosed crustal complex. However, the lower intercept age of 103±14 Ma reported by Putiš et al. (1994, 2000) clearly indicates the age of the main Alpine (Early Cretaceous) higher-temperature metamorphic overprint. The U/Pb lower discordia intercept age of granitic orthogneisses zircon, apatite and monazite is interpreted as cooling of the SSC during exhumation along a deep crustal extension normal detachment fault between 750 - 500 °C (Putiš et al. 2000). These time constraints are consistent with the shortening period in the Meliata-Hallstatt basin passive continental margin (Putiš et al. 2000, 2002).

The Sieggraben structural complex is composed of the following lithological sequences: metapelites (gneisses, micaschists), metabasites (eclogites, amphibolites, metagabbros), metaultramafics (serpentinites), metagranitoids (leucocrate metagranites, metapegmatites), impure metacarbonates and calc-silicate rocks (marbles) (Fig. 2).

Ultramafic rocks of the AA SSC (Kümel 1935; Tollman 1977; Putiš 1992) were most likely affected by eclogite-facies metamorphism together with the hosting gneiss-amphibolite-marble lithological complex containing concordant to discordant veins of granitic-pegmatitic orthogneisses. While the lens shaped metaultramafic bodies were commonly located in the ductile banded amphibolites, they were also found in marbles and gneisses (Putiš et al. 2000, 2002).

The AA SSC rocks indicate two higher-temperature and high-to-medium pressure metamorphic stages; reported here as D1 and D2 deformation stages. D1 denotes burial in a subduction-related wedge and subduction channel, while D2 is a later unroofing and exhumation stage (Putiš et al. 2000, 2002; Kromel et al. 2011). While the D1 prograde burial stage resulted in Omp formation with almost 40 % Jd, Prg-Amp1, Zo, Grt and relics of Pl,

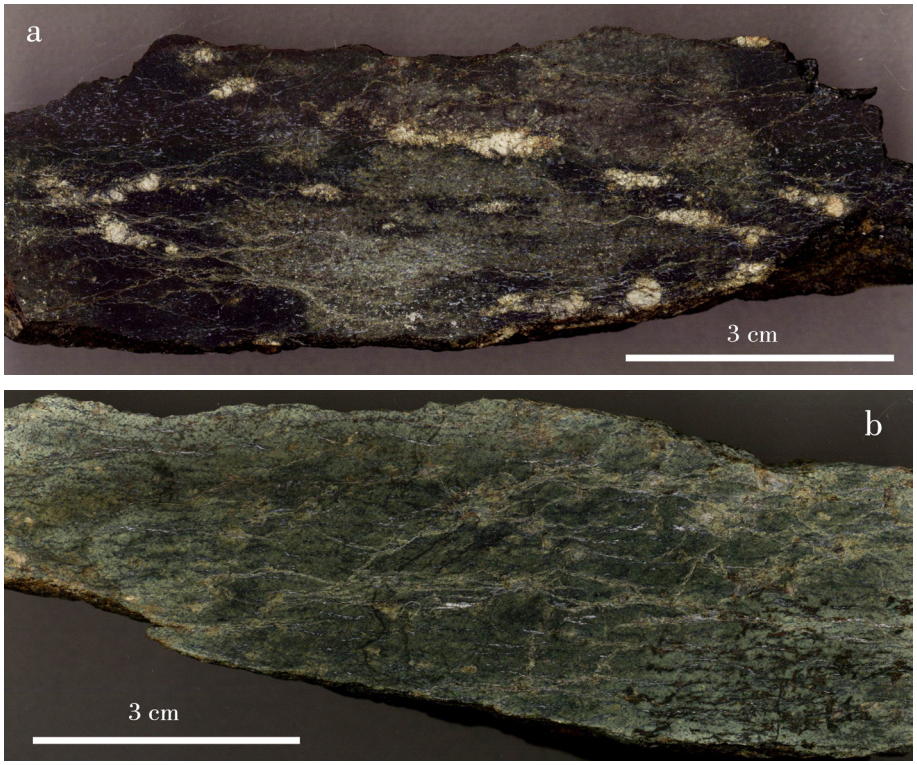

Fig. 3 *Cut surfaces of metaultramafics in the Sieggraben structural complex. The cut is orientated along the mineral stretching-lineation and perpendicular to metamorphic foliation. a) Swarzenbach area sample SW-3-2 with flattened and stretched Opx porphyroclasts in metamorphic foliation, b) Sieggraben area sample S-201-1 with light-coloured aggregates of Chl along schistosity planes. Photo M. Putiš.*

the D2 exhumation stage formed Cpx2-Pl symplectites and Ts-Amp2 coronas around Grt, Pl and Bt (Putiš et al., 2000, 2002).

The D1 temperature had previously been estimated at 610 - 650°C (Grt-Cpx geothermometer) at minimum pressure of 16-17 kbar (Grt-Cpx-Pl-Qz geobarometer) by Kromel et al. (2011). The same authors found D2 P-T at 700°C and 12 kbar by Grt-Bt geothermometer and Grt -Pl-Ky-Qz geobarometer. Compared to model of Putiš et al. (2002), this eclogite-facies metamorphic temperature was estimated slightly lower at higher minimum pressure (Kromel et al. 2011). A brief petrographic characterization of the Sieggraben metaultramafics was reported by Hrvanović et al. (2013a, b).

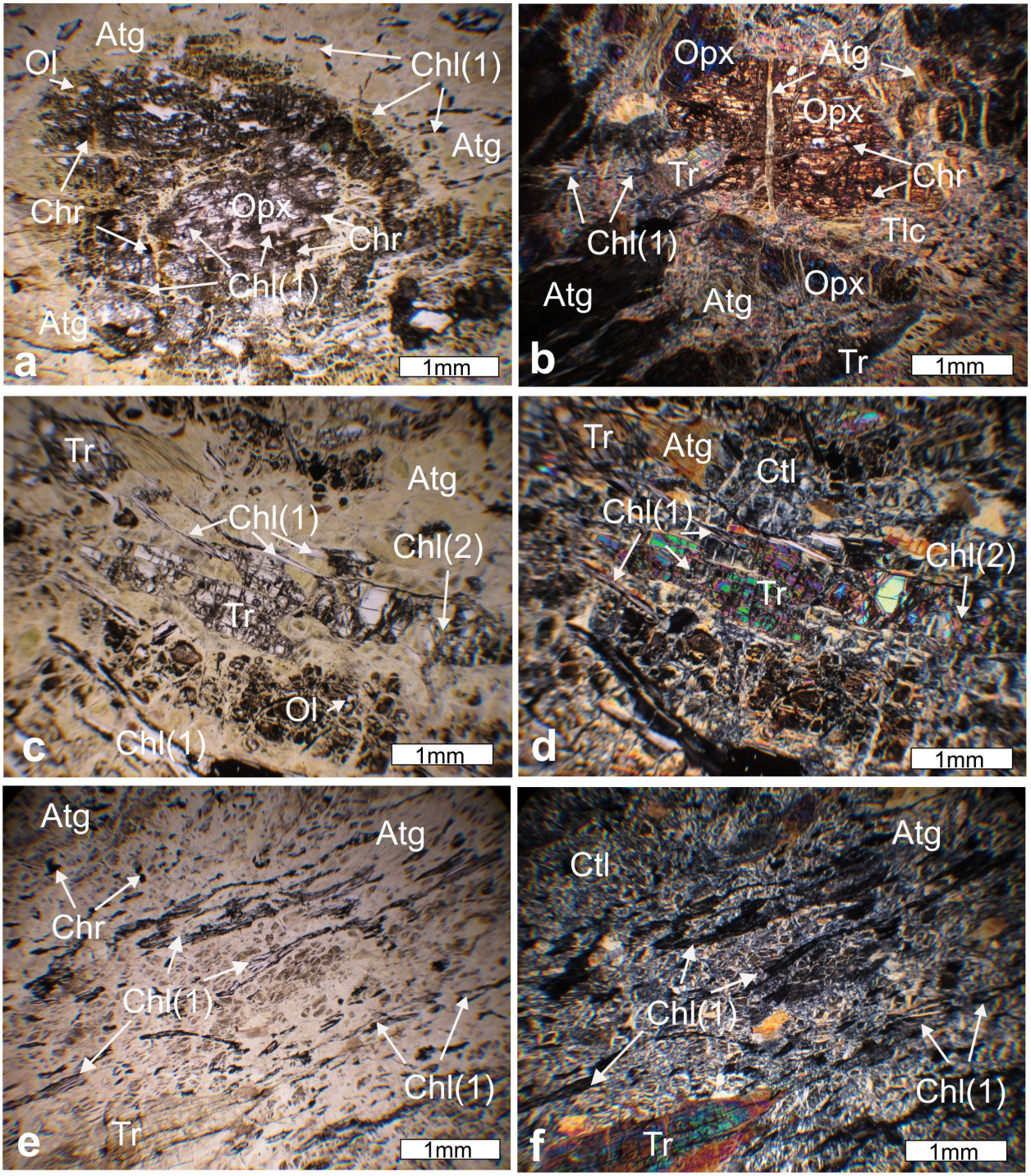

Fig. 4 *Photomicrographs of metaultramafics in the Sieggraben structural complex.*
a) Plain-polarized light microscopic images of Ol, Opx, Atg, Chl (1), Chl (2) and Chr from sample SW-3-1, b) Crossed-polarized light microscopic images of Opx, Chl (1), Tr, Atg and Tlc from sample S-201-2b, c) Plain-polarized light microscopic images of Ol, Atg, Chl (1), Chl (2) and Tr from sample SW-4-1-2c, d) Crossed-polarized light microscopic images of Atg, Chl (1), Chl (2) and Tr in sample SW-4-1-2c, e) Plain-polarized light microscopic images of Atg, Chl (1), Chr and Tr in sample S-201-1, f) Crossed-polarized light of Atg, Chl (1), Ctl and Tr in sample S-201-1. Photo M. Putiš.

Materials and methods

The hand samples listed in Figures 3a and b were collected between Sieggraben and Schwarzenbach villages. Their mineral composition and microstructures were then studied in ten selected polished sections (from 32 sections) by polarized-light microscope Leica DM2500P at the Department of Mineralogy and Petrology, Comenius University in Bratislava.

Chemical compositions of minerals were determined by a Cameca SX-100 electron microprobe at the State Geological Institute of Dionýz Štúr in Bratislava. Analytical conditions were at 15 kV accelerating voltage and 20 nA beam current. Cameca Peak Sight v 4.2 software was used for data recalculation. We used following standards for calibration of the given elements (in brackets): albite (Na), wollastonite (Si, Ca), orthoclase (K), forsterite (Mg), Al_2O_3 (Al), fayalite (Fe), rhodonite (Mn), metallic V, Cr, and Ni, TiO_2 (Ti), $SrTiO_3$ (Sr), $LiNbO_3$ (Nb), $LaPO_4$ (La), $CePO_4$ (Ce), and $LiTaO_3$ (Ta). The beam diameter used was 10 µm.

Mineral formulae were calculated on the basis of 4 Oxygen anions for olivine, 15 (eNK) cations for amphibole, 4 cations for pyroxene, 3 cations for spinel, 14 Oxygen anions for the minerals of serpentine group and chlorite.

Mineral abbreviations used in our text, tables and figures are after Whitney and Evans (2010): Amp = amphibole, Atg = antigorite, Bt = biotite, Chl = chlorite, Chr = chromite, Ctl = chrysotile, Cpx = clinopyroxene, Fa = fayalite, Fo = forsterite, Grt = garnet, Hem = hematite, Jd = jadeite, Ky = kyanite, magnetite = Mag, Ms = muscovite, Omp = omphacite, Ol = olivine, Opx = orthopyroxene, Pl = plagioclase, Prg = pargasite, Qz = quartz, Srp = serpentine group, Tlc = talc, Tr = tremolite, Ts = tschermakite, Zo = zoisite, besides Carb = carbonates.

Results

Metaultramafics exclusively contain metamorphic phases: Opx porphyroblasts (enstatite) in an Ol (forsterite) matrix and Chr associated with Atg, Ctl serpentine minerals, Amp (Tr), Chl, Mag and, very rarely, Tlc.

Chemical analyses were re-calculated for individual mineral phases and their end-member components (Fig. 4). Herein, analytic positions are shown in BSE images (Fig. 5), compositional data is plotted in classification diagrams (Fig. 6) and mineral analysis is listed in Tables 1 - 3.

Petrography and mineral chemistry

Serpentinites from AA SSC occur as lenses in eclogitic amphibolites, gneisses or marbles. Macroscopically, these are (1) massive or slightly schistose with coarse-grained Opx porphyroclasts (0.5 - 1 cm in size; ca. 30 vol. %) randomly oriented in a fine-grained partly serpentinized olivine matrix (approximately 60 vol. %); (2) schistose with preserved flattened and stretched Opx porphyroclasts in Srp minerals and Chl (Fig. 3a) or (3) ranging to di-

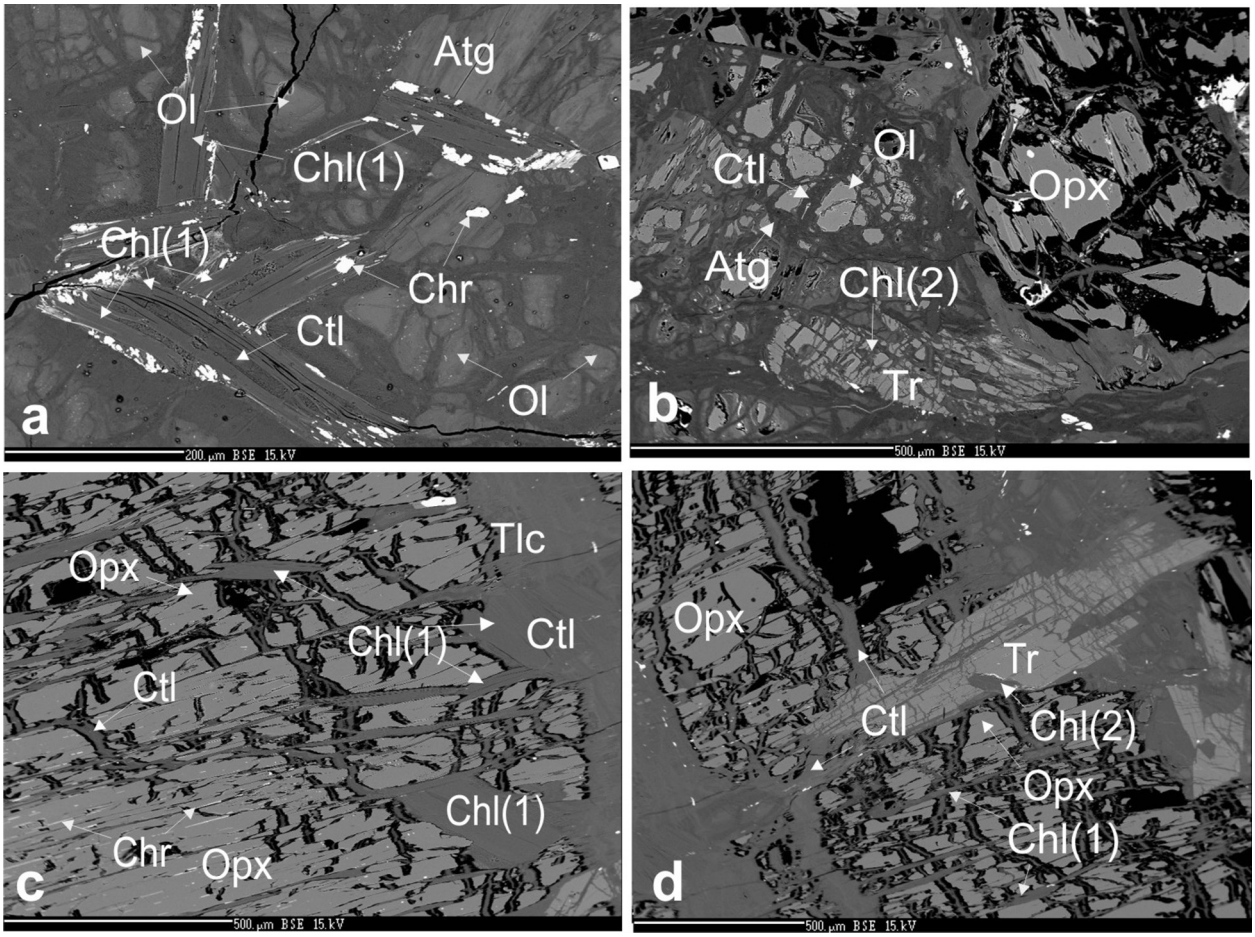

Fig 5 *Back-scattered electron (BSE) images from mineral assemblages of metaultramafics in the Sieggraben structural complex. a) Atg, Chl (1), Ctl, Ol from sample S-200a4, b) Atg, Chl (2), Ol and Opx from sample S-200e, c-d) Chl (1), Chl (2), Chr, Ctl and Opx from sample S-201-2a. Photo I. Holický.*

stinctly schistose without macroscopically preserved Opx porphyroclasts. The latter are almost completely serpentinized with greatest shearing deformation and accompanying serpentinization and chloritization (Fig. 3b).

Polarized light microscopy was used to identify Ol, Opx, spinel group minerals (Chr, around 100 μm in size), Amp (Tr, 100 - 500 μm in size), surrounded by matrix serpentine minerals (coarse-grained Atg 100 - 300 μm in size, and fine-grained Ctl), Chl, and very rarely noted Tlc aggregates and opaque minerals (Mag, Hem) (Fig. 4).

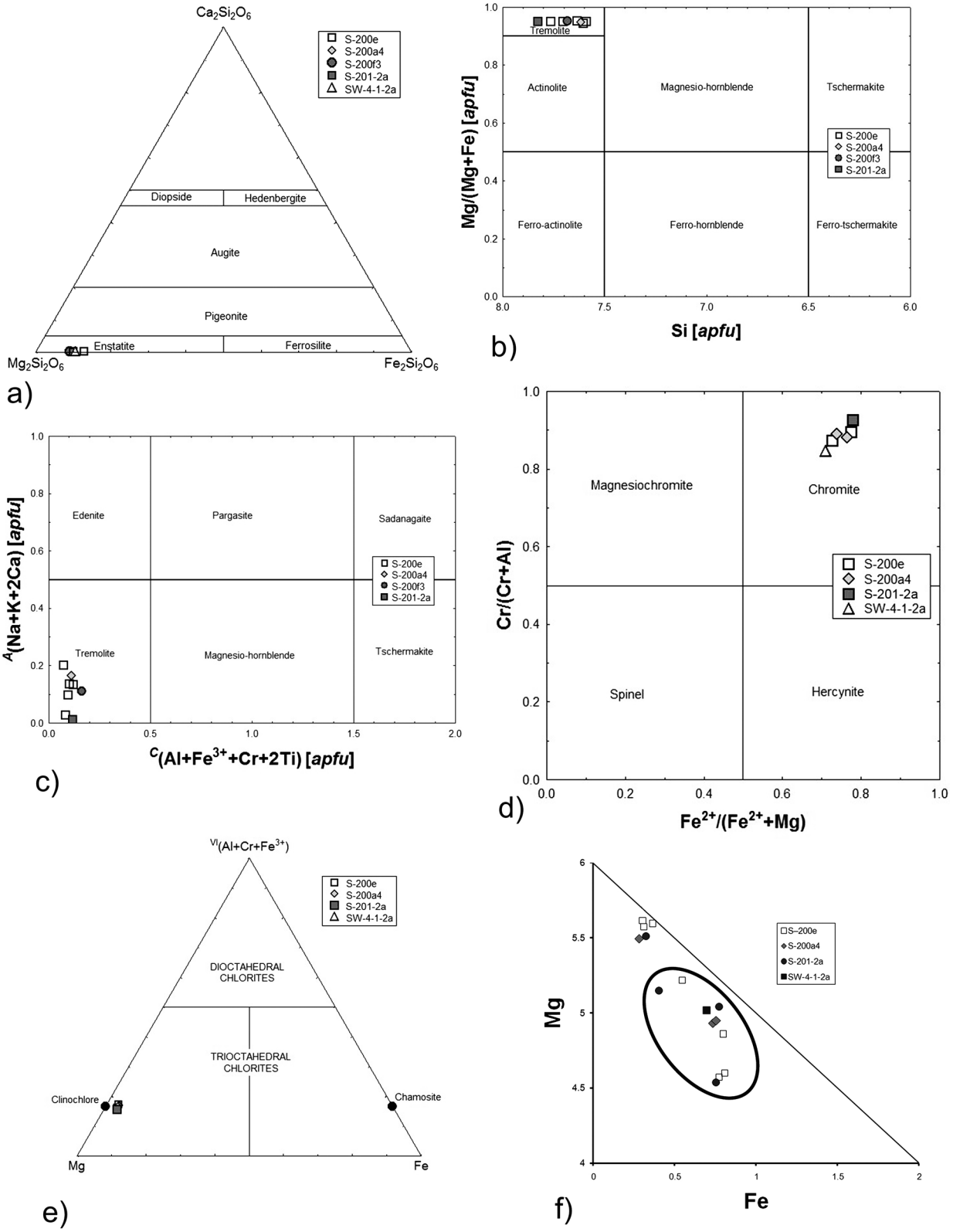

Fig. 6 *Classification diagrams of a) pyroxenes after Morimoto et al. (1988); b) amphiboles after Leake at al. (1997, 2004); c) amphiboles after Hawthorne et al. (2012); d) the spinel group after Lindsley (1991); e) chlorite after Zane and Weiss (1998); f) serpentine group minerals (original diagram).*

Clinopyroxene was not observed in these samples and calcite veinlets were located in only one sample.

Olivine forms aggregates of randomly oriented fine-grained (100 - 10 μm) partly serpentinized matrix with typical mesh structure. The olivine grains show homogeneous chemical composition and have no inclusions (Fig. 4a, Fig. 5a, b). According to the end member composition, Ol contains from 90.38 to 90.51 mol. % of Fo component (Table 1) that is quite characteristic for metamorphic Ol.

The *pyroxene* in our investigated metaultramafics is magnesium-rich low-Al orthopyroxene, enstatite (Fig. 4a, b; Fig. 5b - d; Fig. 6a; Table 1), with Mg ranging from 1.81 to 1.93 *apfu.* It forms coarse-grained relic grains with inclusions of Chr. Orthopyroxene porphyroclasts are partly to totally replaced by Srp minerals (bastite), Chl and Tr. The porphyroclasts show deformation (flattening, stretching and fracturing) due to hydration recrystallization to Srp group minerals and Chl. Dynamic recrystallization was not observed.

Amphibole occurs as prismatic non-pleochroic grains of tremolite (Fig. 4b - d; Fig. 5b, d; Fig. 6b, c). This is well-documented by the analysis recorded here in Table 2. Alteration of amphibole crystals by late serpentine minerals (Ctl) and Chl (2) along cleavage planes is clearly visible in Fig. 4c, d; 5b, d.

Spinel group minerals occur as opaque anhedral grains in the matrix (approximately 5 vol. %) and also as acicular inclusions in Opx. EMPA data defined chromite composition with 1.44 to 1.72 *apfu* Cr-content (Fig. 4a, b; Fig. 5a, c; Fig. 6d; Table 1, 2).

Chlorite forms randomly to strictly oriented flakes in metamorphic schistosity (Figs. 4a - f). Here, two Chl generations can be distinguished. In addition to Srp and Tr presence, the sub-parallel flaky Chl porphyroblasts (1) (usually 100 - 500 μm long grain flakes) define metamorphic schistosity (Fig. 4c - f). Chlorite (1) and Tr overgrow Opx porphyroclasts (Fig. 5a, c, d). In calculated structural formula value, Mg content ranges from 4.7 to 4.8 *apfu* (Table 3). The chemical compositions of Mg-rich Chl (1) are shown in our classification diagram, and these are close to clinochlore (Fig. 6e). Fine-grained aggregates of late generation Mg-rich Chl (2) are alteration products of Ol, Opx and Tr filling fractures in these minerals (Fig. 4b, c; Fig. 5b, d).

Serpentine group minerals occur in the metamorphic matrix or they form pseudomorphs after Ol and Opx (Fig. 4a - f). Our back-scattered electron images show two compositionally different serpentine mineral domains, and these most likely indicate variations in Fe and Mg content (Fig. 5a - d). The Atg flakes have relatively higher Fe content, lower content of octahedral cations and usually lower Si contents than the Ctl fine-grained flaky aggregates (Fig. 6f; Table 3), while chrysotile often ingrows Chl (1) flakes (Fig. 5a). The increased content of Fe with Fe/(Fe+Mg) ratio higher than 0.1 and decreased content of octahedral cations are typical for antigorite in comparison to lizardite (Page 1968).

Talc occurs here as colourless grains with low relief and characteristically high interference colours, and it is subordinately present in the matrix, associated with serpentine group minerals (Fig. 4b; Fig. 5c; Table 2).

Table 1 *Representative mineral analyses of olivine, orthopyroxene and chromite in metaultramafics from the Sieggraben structural complex (wt. %)*

Sample	S-200e	S-201-2a	S-200a4	S-200e	S-200e	SW-4-1-2a
Mineral	Ol	Ol	Opx	Opx	Chr	Chr
Analyses No.	An 25	An 10	An 11	An 5	An 18	An 5
SiO_2	40.94	41.34	57.03	57.81	0.00	0.03
TiO_2	0.00	0.00	0.00	0.00	0.07	0.07
Al_2O_3	0.00	0.00	0.18	0.04	4.85	7.40
V_2O_3	0.00	0.00	0.00	0.00	0.54	0.00
FeO	9.47	9.21	6.39	6.48	28.19	25.72
MnO	0.15	0.16	0.21	0.18	0.66	0.63
MgO	49.70	49.64	35.35	35.54	4.17	5.51
CaO	0.01	0.03	0.11	0.12	0.00	0.03
Na_2O	0.00	0.00	0.00	0.00	0.00	0.00
K_2O	0.01	0.01	0.01	0.01	0.00	0.00
Cr_2O_3	0.01	0.00	0.11	0.02	61.46	60.14
NiO	0.47	0.39	0.10	0.05	0.00	0.02
ZnO	0.00	0.00	0.00	0.00	0.54	0.00
Total	100.76	100.77	99.48	100.25	100.48	99.55
			apfu			
Si^{4+}	0.998	1.007	1.972	1.984	0.000	0.000
Ti^{4+}	0.000	0.000	0.000	0.000	0.002	0.002
Al^{3+}	0.000	0.000	0.007	0.002	0.204	0.302
V^{3+}	0.000	0.000	0.000	0.000	0.000	0.000
Cr^{3+}	0.000	0.000	0.003	0.002	1.721	1.647
Fe^{3+}	0.004	0.000	0.045	0.029	0.075	0.050
Fe^{2+}	0.189	0.187	0.140	0.156	0.760	0.695
Mg^{2+}	1.810	1.802	1.822	1.818	0.219	0.285
Mn^{2+}	0.003	0.003	0.000	0.005	0.019	0.018
Ca^{2+}	0.000	0.001	0.004	0.004	0.000	0.000
Ni^{2+}	0.000	0.000	0.000	0.000	0.000	0.000
Zn^{2+}	0.000	0.000	0.000	0.000	0.000	0.000
Na^{+}	0.000	0.000	0.000	0.000	0.000	0.000
K^{+}	0.000	0.000	0.000	0.000	0.000	0.000
Total	3.000	3.001	3.993	3.998	2.999	2.998
Fo	90.21	90.39				
2Ti/(2Ti+Al+Cr)					0.002	0.002
$2Fe^{3+}/(2Fe^{3+}+Al+Cr)$					0.072	0.048
$Fe^{2+}/(Fe^{2+}+Mg)$					0.776	0.709

Table 2 *Representative chemical composition of amphibole, talc and chromite in metaultramafics from the Sieggraben structural complex (wt. %)*

Sample	S–200e	S-200a4	S-200f3	S-201-2a		S-201-2a	S-201-2a		S-200a4	S-201-2a
Mineral	Amp	Amp	Amp	Amp		Tlc	Tlc		Chr	Chr
Analyses No.	An 20	An 9	An 2	An2		An5	An11		An 12	An 9
SiO_2	56.51	55.64	56.05	57.38	SiO_2	63.45	54.88	SiO_2	0.05	0.06
TiO_2	0.03	0.02	0.01	0.03	TiO_2	0.00	0.00	TiO_2	0.08	0.32
Al_2O_3	2.27	2.68	2.55	1.56	Al_2O_3	0.21	0.03	V_2O_3	0.52	0.40
Cr_2O_3	0.21	0.55	0.62	0.33	V_2O_3	0.00	0.00	Al_2O_3	5.35	2.71
V_2O_3	0.00	0.00	0.00	0.00	FeO	1.65	8.14	FeO	28.90	39.70
Fe_2O_3	0.00	0.00	0.00	0.00	MnO	0.00	0.01	MnO	0.59	0.59
FeO	2.53	2.56	2.38	2.52	MgO	30.97	28.32	MgO	4.35	4.02
MnO	0.08	0.04	0.05	0.06	CaO	0.01	0.66	CaO	0.01	0.02
MgO	23.68	23.35	23.15	23.58	Na_2O	0.08	0.03	Cr_2O_3	59.47	50.71
NiO	0.08	0.22	0.08	0.13	K_20	0.01	0.08	ZnO	0.55	0.35
ZnO	0.00	0.00	0.00	0.00	Cr_2O_3	0.02	0.00	NiO	0.05	0.15
CaO	12.51	12.55	12.64	12.46	NiO	0.06	0.92			
Na_2O	0.97	1.15	0.90	0.56	ZnO	0.00	0.00			
K_2O	0.08	0.11	0.09	0.07						
Total	98.95	98.87	98.52	98.67	Total	96.46	93.07	Total	99.92	99.02
Si^{4+}	7.703	7.616	7.681	7.826	Si^{4+}	3.984	3.702	Ti^{4+}	0.002	0.009
$Al_{3+}T$	0.297	0.384	0.318	0.174	Ti^{4+}	0.000	0.000	Al^{3+}	0.233	0.115
T-sum.	8.000	8.000	8.000	8.000	Al^{3+}	0.015	0.002	Cr^{3+}	1.668	1.443
Ti^{4+}	0.003	0.002	0.001	0.003	V^{3+}	0.000	0.000	Fe^{3+}	0.107	0.434
$Al^{3+}Z$	0.067	0.049	0.094	0.076	Fe^{3+}	0.000	0.000	Fe^{2+}	0.751	0.761
Cr^{3+}	0.023	0.060	0.067	0.036	Fe^{2+}	0.087	0.459	Mg^{2+}	0.230	0.216
V^{3+}	0.000	0.000	0.000	0.000	Mn^{2+}	0.000	0.000	Mn^{2+}	0.018	0.018
Mg^{2+}	4.812	4.765	4.772	4.793	Mg^{2+}	2.899	2.849	Total	3.009	2.995
Mn^{2+}	0.009	0.005	0.006	0.007	Ca^{2+}	0.001	0.047			
Fe^{3+}	0.000	0.000	0.000	0.000	Na^{+}	0.010	0.004			
Fe^{2+}	0.250	0.240	0.237	0.249	K^{+}	0.001	0.007			
Zn^{2+}	0.000	0.000	0.000	0.000	Cr^{3+}	0.001	0.000			
Ni^{2+}	0.009	0.025	0.009	0.015	Ni^{2+}	0.000	0.000			
C-sum.	5.173	5.159	5.144	5.179	Zn^{2+}	0.000	0.000			
Ca^{2+}	1.827	1.841	1.856	1.821	Total	6.996	7.071			
Na^{+}	0.173	0.159	0.144	0.148						
B-sum.	2.000	2.000	2.000	1.969				2Ti/(2Ti+Al+Cr)	0.002	0.011
Na^{+}	0.083	0.146	0.095	0.000				$2Fe^{3+}/(2Fe^{3+}+Al+Cr)$	0.101	0.358
K^{+}	0.014	0.019	0.016	0.012				$Fe^{2+}/(Fe^{2+}+Mg)$	0.765	0.779
A-sum.	0.097	0.165	0.111	0.012				Cr/(Cr+Al)	0.882	0.926

Discussion

Austroalpine SSC metaultramafics are mostly intensively serpentinized, with no preserved relics of primary magmatic minerals. The metamorphic mineral compositions indicate a harzburgite-type peridotite protolith, typical of the sub-continental mantle lithosphere (Arai 1994; Bodinier, Godard 2007).

The AA SSC shows three deformation-recrystallization stages (D1 to D3) according to Putiš et al. (2000, 2002) and Kromel et al. (2011). Our studied serpentinites demonstrate the following three metamorphic stages; (1) The prograde metamorphic stage (D1) defined by inferred HT/HP metamorphic mineral assemblage of Ol (with increased Fa component) and low-Al Opx, most likely due to eclogite facies metamorphic conditions; (2) The assemblage of Atg, Tr, Mg-Chl (1) and Chr provides the MT amphibolite facies retrograde stage (D2), and (3) The assemblage of Ctl, Mg-Chl (2), Mag, ±Tlc and ±Carb indicates the LT or greenschist facies (Bucher, Grapes 2011) retrograde metamorphic conditions of the inferred D3 exhumation stage. Finally, the deformation structures are mainly related to MT/LT D2 and D3 exhumation stages connected with hydration of Ol and Opx and their replacement by Srp minerals and Chl.

The P-T conditions of the inferred metamorphic facies have been reported by both Putiš et al. (2002) and Kromel et al. (2011). However, their P-T estimates were not obtained from the same rocks presented here. Although the mineral composition (Grt-free) of the studied metaultramafics is not suitable for geothermobarometric estimates, the mineral assemblages of the D1 to D3 metamorphic

Table 3 *Representative mineral analyses of Atg, Ctl and Chl in metaultramafics from the Sieggraben structural complex (wt. %)*

Sample	S-200e	S-201-2a	S-200e	S-200a4	S-200a4	S-200a4	S-201-2a	SW-4-1-2a
Mineral	Atg	Atg	Ctl	Ctl	Atg	Chl(1)	Chl(2)	Chl(1)
Analyses No.	An 1	An 14	An 2	An 4	An 6	An 3	An3	An3
SiO_2	40.19	40.28	42.63	43.65	41.23	32.40	34.09	31.70
TiO_2	0.00	0.01	0.00	0.01	0.00	0.00	0.01	0.02
Al_2O_3	0.24	0.01	0.04	0.04	0.13	14.30	12.77	14.31
Cr_2O_3	0.06	0.02	0.00	0.03	0.09	3.53	3.72	2.66
V_2O_3	0.00	0.00	0.00	0.00	0.00	0.00	0.00	0.00
Fe_2O_3	0.00	0.00	0.00	0.00	0.00	0.00	0.00	0.00
FeO	9.29	9.19	3.95	3.61	8.76	2.79	2.99	2.92
MnO	0.08	0.29	0.04	0.15	0.07	0.02	0.04	0.06
MgO	31.70	33.60	39.48	39.29	33.00	33.68	33.77	31.70
NiO	0.13	0.43	0.33	0.05	0.14	0.25	0.27	0.20
ZnO	0.00	0.00	0.00	0.00	0.00	0.00	0.00	0.00
CaO	0.11	0.04	0.04	0.03	0.15	0.00	0.03	0.01
Na_2O	0.01	0.04	0.00	0.00	0.00	0.01	0.00	0.07
K_2O	0.02	0.01	0.00	0.01	0.00	0.00	0.01	0.00
Total	81.83	83.91	86.51	86.87	83.57	86.98	87.71	83.66
					apfu			
Si^{4+}	4.131	4.055	4.037	4.095	4.133	3.085	3.218	3.128
$^{IV}Al^{3+}$	0.000	0.000	0.000	0.000	0.000	0.915	0.782	0.872
T-sum.	4.131	4.055	4.037	4.095	4.133	4.000	4.000	4.000
Ti^{4+}	0.000	0.001	0.000	0.001	0.000	0.000	0.000	0.001
$^{VI}Al^{3+}$	0.029	0.001	0.004	0.004	0.015	0.689	0.638	0.792
Cr^{3+}	0.005	0.001	0.000	0.002	0.007	0.266	0.277	0.208
V^{3+}	0.000	0.000	0.000	0.000	0.000	0.000	0.000	0.000
Fe^{2+}	0.798	0.773	0.313	0.283	0.734	0.222	0.236	0.241
Mn^{2+}	0.007	0.024	0.003	0.012	0.006	0.002	0.003	0.005
Mg^{2+}	4.857	5.041	5.573	5.495	4.932	4.780	4.751	4.662
Zn^{2+}	0.000	0.000	0.000	0.000	0.000	0.000	0.000	0.000
Ni^{2+}	0.011	0.036	0.026	0.004	0.012	0.020	0.022	0.017
Ca^{2+}	0.012	0.005	0.004	0.003	0.016	0.000	0.003	0.001
Na^{+}	0.002	0.007	0.000	0.000	0.000	0.002	0.000	0.014
K^{+}	0.003	0.001	0.000	0.001	0.000	0.000	0.001	0.000
M-sum.	5.724	5.892	5.924	5.806	5.723	5.981	5.933	5.942

stages suggest a common tectonometamorphic evolution of metaultramafics with the hosting eclogite facies rocks; following the subductional burial D1 phase and during the D2 and D3 exhumation stages. Garnet-free lithologies indicate the maximum subduction pressures (D1) of these metaultramafics at approximately 20 kbars. The presence of Ol+Opx, however, indicates the higher D1 temperatures of 600 - 750°C deduced from the petrogenetic grid (Bucher, Grapes 2011).

Conclusions

While the investigated rocks contain no primary magmatic minerals, the Ol (enriched in Fa) and Opx (Al-poor) chemical compositions clearly indicate their metamorphic origin. The predominating metamorphic olivine-orthopyroxene composition was most likely inherited from harzburgitic protoliths.

Olivine (forsterite) and orthopyroxene (enstatite) rich relics indicate the inferred eclogite facies metamorphic stage (D1; with estimated temperature of 600 - 750°C at approximately 15 - 20 kbar pressure deduced from the petrogenetic grid). The superimposed mineral assemblage of antigorite, tremolite, Mg-rich chlorite (1) and chromite forming the metamorphic matrix provide the exhumation amphibolite facies metamorphic stage (D2); and chrysotile, Mg-rich chlorite (2), magnetite, rare talc and carbonates determine the greenschist facies metamorphic stage (D3).

Metaultramafics from the Sieggraben structural complex are fragments of metaperidotites, attached to the subducted lower continental crust during the Cretaceous tectonometamorphic event also reported in other areas of the Eastern Alps Austroalpine basement.

Acknowledgements

This work was supported by APVV-0081-10 and VEGA-1/0255/11 scientific grants (M.P.). Suggestions of G. Habler (Vienna University) and P. Siman (Slovak Academy of Sciences in Bratislava) are greatly acknowledged. We also thank R. Marshall for reviewing the English content.

References

Arai S. (1994) Characterization of spinel peridotites by olivine-spinel compositional relationships: review and interpretation. *Chem. Geol. 113, 191-204.*

Bodinier J. L., Godard M. (2007) Orogenic, Ophiolitic, and Abyssal Peridotites. *TrGeo 2.04, 1-73.*

Bucher K., Grapes R. (2011) Petrogenesis of Metamorphic Rocks. *Springer-Verlag, Berlin, Heidelberg, 8th ed., 1-428.*

Dallmeyer R. D., Neubauer F., Handler R., Fritz H., Muller W., Pana D., Putiš M. (1996) Tectonothermal evolution of the internal Alps and Carpathians: evidence from 40Ar/39Ar mineral and whole-rock data. *Eclogae Geol. Helv. 89, 1, 203-227.*

Dallmeyer R. D., Neubauer F., Handler R., Muller W., Fritz H., Antonitsch W., Hermann S. (1992) 40Ar/39Ar and Rb-Sr mineral age controls for the Pre-Alpine and Alpine tectonic evolution of the Austro-Alpine napple complex, Eastern Alps. *In: Neubauer F. (Ed.): ALCAPA-Field Guide, University Graz, 47-59.*

Frank W., Kralik M., Scharbert S., Thöni M. (1987) Geochronological data from the Eastern Alps. *In: Flugel H. W., Faupl P. (Eds.): Geodynamics of the Eastern Alps. F. Deuticke, Vienna, 272-281.*

Frisch W., Neubauer F. (1989) Pre-Alpine terrenes and tectonic zoning in the Eastern Alps. *In:* Dallmayer R.D. (Ed.): Terranes in the Circum-Atlantic Paleozoic orogens. Special Paper, *Geol. Soc. Am. 230, 91-100.*

Froitzheim N., Schmid S. M., Frey M. (1996) Mesozoic paleogeography and the timing of eclogite-facies metamorphism in the Alps: A working hypothesis. *Eclogae Geol. Helv. 89, 81-110.*

Hawthorne C. F., Oberti R., Harlow G., Maresch V. W., Schumaher C. J., Welch M. (2012) Nomenclature of the amphibole supergroup. *Am. Mineral. 97, 2031-2048.*

Hrvanović S., Putiš M., Bačík P. (2013a) Metaultramafics in the eclogitic Sieggraben complex (Eastern Alps), *Univerzita Komenského v Bratislave, Prírodovedecká fakulta, Študentská vedecká konferencia PriF UK 2013. Zborník recenzovaných príspevkov.1253-1258.*

Hrvanović S., Putiš M., Bačík P., Kromel J. (2013b) Petrological characterization of metaultramafics in the Sieggraben complex (Eastern Alps). *Univerzita Komenského v Bratislave, MINPET 2013.*

Korikovsky S. P., Putiš M., Kotov A. B., Salnikova E. B., Kovach V. P. (1998) High-pressure metamorphism of the phengite gneisses of the Lower Austroalpine nappe complex in the Eastern Alps: mineral equilibria, P-T parameters, and age. *Petrology 6, 603-619.*

Kromel J., Putiš M., Bačík P. (2011) The Middle Austro -Alpine Sieggraben structural complex - new data on geothermobarometry. *Acta Geol. Slovaca 3, 1-12.*

Kümel F. (1935) Die Sieggrabener Deckscholle im Rosaliengebirge (Nieder Österreich-Burgenland). *Tschermaks Mineral. Petrogr. Mitt. 47, 141-184.*

Leake B. E., Woolley A. R., Arps C. E. S., Birch W. D., Gilbert M. C., Grice J. D., Hawthorne F. C., Kato A., Kisch H. J., Krivovichev V. G., Linthout K., Laird J., Mandarino J. A., Maresch W. V., Nickel E. H., Schumacher J. C., Smith D. C., Stephenson N. C. N., Ungaretti L., Whittaker E. J. W., Youzhi G. (1997) Nomenclature of Amphiboles. *Can. Mineral. 35, 219-246.*

Leake B. E., Woolley A. R., Birch W. D., Burke E. A. J., Ferraris G., Grice J. D., Hawthorne F. C., Kisch H. J., Krivovichev V. G., Schumacher J. C., Stephenson N. C. N., Whittaker E. J. W. (2004) Nomenclature of amphiboles: Additions and revisions to the International Mineralogical Association's amphibole nomenclature. *Am. Mineral. 89, 883-887.*

Lindsley D. H. (1991) Oxide minerals: petrologic and magnetic significance. *Rev. Mineral. 25, 509 pp.*

Matte P. (1986) Tectonics and plate tectonics model for the Variscan belt of Europe. *Tectonophysics 126, 2-4, 329-374.*

Matte P. (1991) Accretionary history and crustal evolution of the Variscan Belt in Western Europe. *Tectonophysics 196, 3-4, 309-337.*

Morimoto N., Fabries J., Ferguson A. K., Ginzburg I. V., Ross M., Seifert F. A., Zussman J. (1988) Nomenclature of pyroxenes. *Am. Mineral. 73, 1123-1133.*

Neubauer F. (1994) Kontinentkollision in den Ostalpen. *Geowiss. 12, 136-140.*

Neubauer F., Frisch W. (1993) The Austro-Alpine metamorphic basement east of the Tauern Window. *In: von Raumer J. F., Neubauer F. (Eds.): The Pre-Mesozoic geology of the Alps. Springer Verlag, Heidelberg, 515-535.*

Neubauer F., Müller W., Peindl P., Mozschewitz E., Wallbrecher E., Thöni M. (1992) Evolution of lower Austroalpine units along the eastern margins of the Alps: a review. *In: Neubauer F. (Ed.): ALCAPA-Field Guide. University Graz, 97-114.*

Page N. J. (1968) Chemical differences among the serpentine "polymorphs". *Am. Mineral. 53, 201-201.*

Putiš M. (1992) Bericht 1991 Über geologische Aufnahmen im kristallinen Grundgebirge auf Blatt 107 Mattersburg. *Jahrb. Geol. Bundesanst. 135, 725-726.*

Putiš M., Korikovsky S. P. (1993) From subduction to uplift history: metamorphism, thrust and extensional tectonics of the Sieggraben unit, E. Alps. *Terra abstracts, Abstract Supplement No. 2 to Terra Nova 5, 28.*

Putiš M., Korikovsky S. P. (1995) Rheological/petrological path of the eclogite-, marble-, gneiss-bearing complexes during extensional uplift (the Sieggraben unit, Middle Austroalpine, Eastern Alps). *In: Schulmann K., Vrána S. (Eds.): Thermal and Mechanical Interactions in Deep Seated Rocks, Journal of the Czech Geological Society, Abstract 40, 3, 38-39.*

Putiš M., Korikovsky S. P., Pushkarev Y. D. (2000) Petrotectonics of an Austroalpine eclogite-bearing complex (Sieggraben, Eastern Alps) and U-Pb dating of exhumation. *Jahrb. Geol. Bundesanst. 142, 73-93.*

Putiš M., Korikovsky S. P., Pushkarev Y. D., Zakariadze G. S. (1994) Geology, tectonics, petrology, geochemistry and isotope dating of the Sieggraben (Grobgneis and Wechsel) Unit in the Eastern Alps. *Manuscript, Geological Survey of Austria, Vienna, 154 p.*

Putiš M., Korikovsky S. P., Wallbrecher E., Unzog W., Olesen N. O., Fritz H. (2002) Evolution of an eclogitized continental fragment in the Eastern Alps (Sieggraben, Austria). *J. Struct. Geol. 24, 2, 339-357.*

Schmid M., Fügenschuh B., Kissling E., Schuster R. (2004) Tectonic map and overall architecture of the Alpine orogen. *Eclogae geol. Helv. 97, 93-117.*

Thöni M., Jagoutz E. (1993) Isotopic constraints for eo-Alpine high-P metamorphism in the Austroalpine nappes of the Eastern Alps: Its Bearing on Alpine orogenesis. *Schweiz. Mineral. Petrogr. Mitt. 73, 177-189.*

Tollmann A. (1977) Geologie von Österreich. Band I: Die Zentralalpen. *Deuticke, Vienna.*

Tollmann A. (1980) Geology and tectonics of the Eastern Alps (Middle Sector). *Abh. Geol. Bundesanst. Wien 34, 197-255.*

Whitney D. L., Evans B. W. (2010) Abbreviations for names of rock-forming minerals. *Am. Mineral. 95, 185-187.*

Zane A., Weiss Z. (1998) A procedure for classifying rock-forming chlorites based on microprobe data. *Rend. Fis. Acc. Lincei 9, 1, 51-56.*